

About Fluids Structure in Microchannels

Rudyak V.Ya.^{*1}, Belkin A.A.², Egorov V.V.³, Ivanov D.A.⁴

Novosibirsk State University of Architecture and Civil Engineering,
630008, Leningradskaya str., 113, Novosibirsk, Russia

¹valery.rudyak@mail.ru, ²a_belkin@ngs.ru, ³v.v.egorov@bk.ru,

⁴divanov@list.ru

ABSTRACT

The paper deals with molecular dynamics simulation of fluid flow characteristics in nanochannels. A new MD algorithm is developed to simulate plane flow with a pressure drop along the channel. Fluids of hard spheres and Lennard-Jones molecules are considered. Emphasis is on the study of the dependence of the hydraulic flow resistance on the fluid structure. An analysis was made of (i) the density distribution across and along the channel; (ii) radial distribution function of the fluid near the channel wall and in bulk; (iii) influence of the interaction law of the molecules with the wall; (iv) the dependence of the flow resistance coefficient on the Reynolds and Knudsen numbers.

1. INTRODUCTION

Flows in microchannels have long attracted the attention of researchers. This is due to the wide occurrence of such flows. They occur in various wildlife objects as well as in various natural porous media. In recent decades, interest in microflows has increased because of various technological applications (catalytic systems, micropower systems, microelectromechanical systems for various applications, nanotechnologies, etc.). For obvious reasons, such flows are difficult, or even impossible, to study experimentally. At best, it is possible to obtain information on some integral characteristics (flow rate, pressure drop, average velocity, etc.). However, even such data can be obtained only in large microchannels. A feasible method for obtaining information on flow in smaller-size channels is molecular dynamics (MD) simulation. The first MD simulations were carried out more than twenty years ago (see [1] and the references therein). Directional motion of a fluid in a nanochannel is usually produced by using an artificial external mass force. This force is often called the gravitational force, but it is hundreds times higher than the characteristic values of gravity. Because the action of the external force leads to a continuous increase in the molecules velocity and temperature, it is necessary to additionally stabilize the system. This is done by using the so-called thermostat method, which, in essence, is a numerical technique that does not have a real physical analog. The introduction of such a mass force is not suitable for simulating real microflows generated by a pressure difference along the channel or a specified flow rate at the entrance. This technique does not allow one to study the pressure drop along the channel and the resistance on the wall. The purpose of the present work is to simulate real flow in a nanochannel with a pressure gradient using the MD method. A new MD algorithm for simulating this flow is proposed, and the flow characteristics and the fluid structure in the nanochannel are analyzed.

* Corresponding author. Tel.: +7 3832668014; valery.rudyak@mail.ru

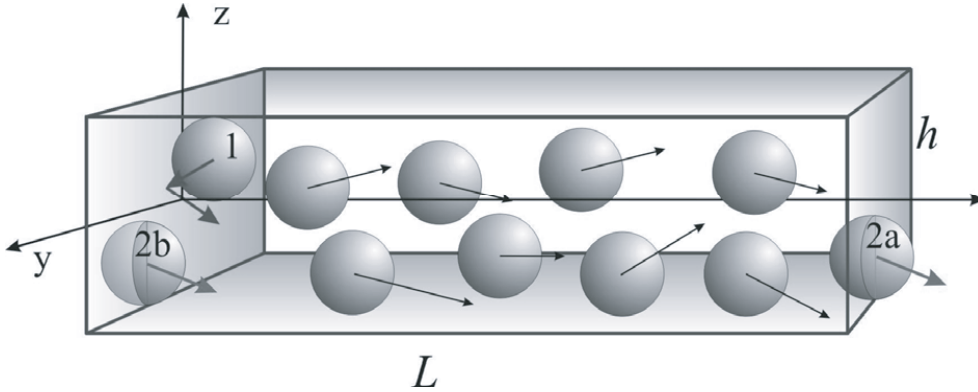


Figure 1. Diagram of plane flow simulation with pseudo-periodic boundary conditions

2. MD SIMULATION TECHNIQUE

Plane Poiseuille flow was modeled in a nanochannel between two solid parallel plates of infinite width (see Figure 1). The simulation cell was a rectangular parallelepiped. The lower and upper faces of the parallelepiped (perpendicular to the z axis) are the channel walls. Along the y axis, the usual periodic boundary conditions [1] are specified which allow the system to be considered infinite in this direction. Nevertheless, the simulation cell size in this direction (width of the cell) is a finite quantity.

The fluid moves in the channel from left to right along the x axis. To implement the flow, we developed a technique which uses specially modified periodic boundary conditions on the left and right faces of the cell. The molecules in the channel cannot penetrate through the left face of the cell (molecule 1 in Figure 1), and interaction with this face is specified by specular or diffuse boundary conditions (described below). The right face is open to the molecules; when a molecule penetrates through the upper boundary (molecule 2a in Figure 1), a copy of this molecule is created on the left boundary (molecule 2b). The x coordinates of the centers of the molecule and copy differ by the channel length L , and their remaining coordinates and velocities are identical. The equations of motion for such a molecule are solved taking into account its interactions with the molecules at both the left and right boundaries, in agreement with the periodic boundary conditions. When a molecule crossing the right boundary of the cell leaves the channel, the copy at the left face remains. Its velocity is randomly recalculated according to the Maxwell distribution

$$f(v_i) = \sqrt{\frac{m}{2\pi kT}} \exp\left(-\frac{mv_i^2}{2kT}\right), \quad i = x, y, z, \quad f(v) = 4\pi \left(\frac{m}{2\pi kT}\right)^{\frac{3}{2}} v^2 \exp\left(-\frac{mv^2}{2kT}\right), \quad (1)$$

where T is the temperature of the left wall, m is the molecule mass, and v and v_i are the absolute value and projection of the molecule velocity. The projection of the molecular velocity onto the x axis is always defined positively. Thus, the left boundary of the channel can be treated as a source of molecules distributed according to eqn (1). In the simulation algorithm considered, the total number of molecules in the cell remains constant, which is convenient for the software implementation of the algorithm.

The truncated Lennard-Jones (LJ) potential

$$\Phi(r) = 4\varepsilon \left(\left(\frac{\sigma}{r} \right)^{12} - \left(\frac{\sigma}{r} \right)^6 \right) \quad (2)$$

or the elastic hard sphere (HS) potential

$$\Phi(r) = \begin{cases} \infty, & r \leq d \\ 0, & r > d \end{cases} \quad (3)$$

are used to describe the interaction of the fluid molecules. Here σ and ε are the parameters of LJ potential and d is the diameter of hard sphere. Each of these two potentials corresponded to a particular method of modeling the interaction between the fluid molecules and the channel walls. For flow of LJ molecules, each wall was modeled by two rows of immobile molecules located at the nodes of a face-centered cubic close packing. The interaction of the fluid molecules with the molecules of the walls was defined by the LJ potential with the parameters $\sigma_{12} = \sqrt{\sigma_{11}\sigma_{22}}$ and $\varepsilon_{12} = \sqrt{\varepsilon_{11}\varepsilon_{22}}$, where σ_{11} , ε_{11} and σ_{22} , ε_{22} are the interaction parameters for the fluid and walls molecules, respectively. In this work, argon flow between carbon walls was studied. The following potential parameters were used: $\sigma_{11} = 3.405 \text{ \AA}$ and $\varepsilon_{11}/k = 119.8 \text{ }^\circ\text{K}$ for argon molecules [2] and $\sigma_{22} = 3.4 \text{ \AA}$ and $\varepsilon_{22}/k = 28 \text{ }^\circ\text{K}$ for carbon molecules [3].

For flow of HS fluid, the upper and lower walls of the channel were modeled by two homogeneous parallel solid surfaces. The interaction of molecules with the surfaces was described by specular, diffuse or specular-diffuse laws of reflection. In the case of specular reflection, the tangential component of the molecular velocity remained constant, and the normal component was reversed. For diffuse reflection, the molecular velocity after collision with the wall was given by a Maxwell distribution (1). During specular-diffuse reflection, a fraction θ of the molecules is diffusely reflected, and the others are specularly reflected. We note that the specular boundary conditions correspond to the zero coefficient of momentum accommodation by the walls, and the accommodation coefficient of diffuse walls is maximal and equal to unity.

At the initial time, the fluid molecules were uniformly arranged in a simulation cell. Their density was determined by the Van der Waals parameter $\varepsilon_v = n\sigma^3$, where n is the number density of the molecules and σ is their diameter determined from relations (2), (3). Velocities at the initial time were specified according to the Maxwell distribution (1). After that, the evolution of the system was calculated. The Schofield scheme [4] was used for the system of LJ molecules, and the standard MD simulation algorithm was used for HS molecules [1, 5]. The time integration step was set equal to $\Delta t = 10^{-12}$ sec. The effective range of the potential was $R = 2.35\sigma$ in all calculations. After the completion of the relaxation processes, whose time depends on the channel length L and height h , fluid density, conditions of interaction with the walls, steady-state flow was established in the channel. Next, the required characteristics were calculated.

3. FLOW CHARACTERISTICS IN NANOCANNELS

The MD algorithm described here allows modeling of plane fluid flow with a pressure gradient along the channel. The characteristics of this flow and their dependence on the fluid molecules interactions with the walls will be analyzed in this section. In all cases, nanoflows were studied. The channel height was varied from 6 to 50 molecule diameters, the channel

length was varied from 60 to 250 molecule diameters, and the width from 6 to 20 molecule diameters. Thus, the longest channel had length slightly greater than 70 nm. The fluid density was varied over a rather wide range: $\varepsilon_v = 0.0014 \div 0.88$.

3.1. THE FLOW VELOCITY PROFILE

The flow velocity profile depends on the interaction law of the fluid molecules with the wall. The parabolic velocity profile

$$u = A(z^2 - zh - \delta h) \quad (4)$$

is formed for LJ fluid. Here A is a constant and δ is the slip length. The slip effect for LJ fluid flow has been observed previously [1]. The flow of HS fluid is first modeled. In this case, a parabolic velocity profile of type (4) is obtained only if the interaction between the fluid molecules and the wall is not specular. The slip length increases with decreasing accommodation coefficient, and during specular interaction with the boundaries, it tends to infinity. Thus, a shock velocity profile for the fluid velocity along the channel is observed for the specular reflection of the molecules.

The velocity on the wall for a macroscopic liquid flow is equal to the wall velocity; the no-slip boundary condition is satisfied. Slip occurs only for rarefied gas flows. In this case the slip length $\delta \sim l \sim Kn$ [6], where l is the molecule free path length and Kn is the Knudsen number. It is considered that slip should be taken into account beginning from a Knudsen number $Kn \sim 5 \cdot 10^{-3}$. The nature of the slip effect in liquid flows is much more complex than that for a gas flow. From a kinetic point of view, the slip length in the liquid flows should be of the order of σ or less. However in experiments, the slip length was found to range from a few nanometers to twenty microns [7]. This length can be greater if the special hydrophobic or ultrahydrophobic skins are used [8, 9]. It is clear that this fact is in contradiction to the kinetic theory.

For a LJ fluid, the slip length depends on the interaction potential between the fluid and wall molecules and on the fluid density. In the calculations performed, the slip length decreased with increasing density (so that $\delta = 0.31d$ at $\varepsilon_v = 0.79$ and $\delta = 0.81d$ at $\varepsilon_v = 0.28$).

The slip length of a HS fluid is primarily determined by the accommodation coefficient. It increases with decreasing the accommodation coefficient. For example, the slip length is equal to $1.7d$ when the accommodation coefficient is equal to $\theta = 0.5$ (the fluid density $\varepsilon_v = 0.88$), but this length is equal to $0.5d$ when $\theta = 1$. Naturally, decreasing fluid density leads to an increase in slip length. In gas flow of density $\varepsilon_v = 0.0014$, the slip length is about $10d$.

3.2. FLOW RATE AND FRICTION COEFFICIENT

The flow rate is the major characteristics of the usual Poiseuille flow. MD algorithm developed in this study does not allow specifying the flow rate at the channel entrance. It is generated during the flow evolution and depends on the channel geometry and the interaction law of the molecules with the walls. However this algorithm realizes flow with a linear pressure gradient along the channel. The value of this gradient is determined primarily by the interaction potential parameters of the fluid and walls molecules. Figure 2 gives a typical pressure drop along the channel for various types of interaction of fluid molecules with each other and with the channel walls; the pressure is normalized by the corresponding quantity at the channel entrance. The pressure drop is equal to zero for the specular reflection of the molecules (the line 1). In case of specular-diffuse reflection of the fluid molecules from the walls the fluid pressure decreases linearly along the channel, i.e., the pressure gradient remains constant (line 2). For a LJ fluid, the pressure also decreases linearly (curve 3). The

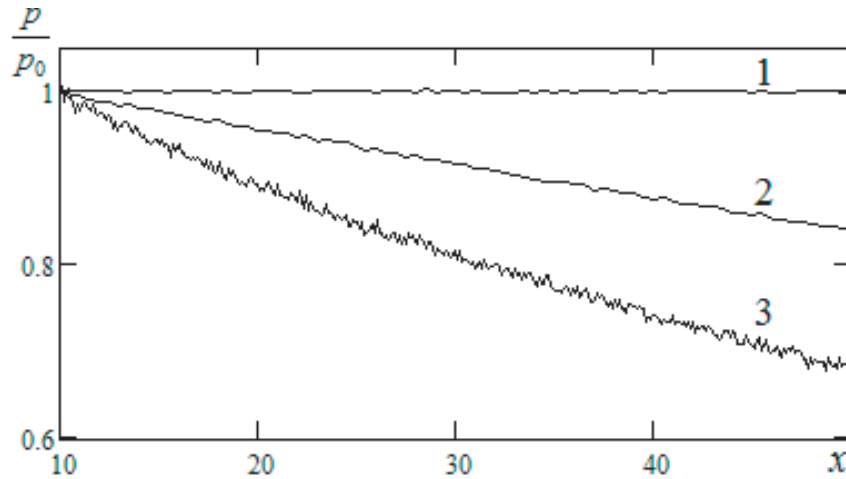


Figure 2. Pressure versus longitudinal coordinate of the channel. 1 – HS fluid, $\theta = 0$; 2 – HS fluid, $\theta = 0.5$; 3 – LJ fluid. In all cases, $L = 60\sigma$, $h = 6\sigma$, $\varepsilon_v = 0.79$

pressure drop along the channel is related to the resistance due to the interaction of the molecules with the walls. The value of pressure drop increases with increasing the accommodation coefficient.

Along with the flow rate, an important flow characteristic is the hydraulic resistance coefficient given by the Darcy–Weisbach formula [10]

$$\lambda = h \frac{dp}{dx} \frac{2}{\rho \bar{u}^2}$$

which contains the average flow velocity $\bar{u} = Q/p$, where Q is the flow rate. In classical hydrodynamics, this flow rate is proportional to the pressure gradient

$$Q = \frac{1}{S} \int_0^h \rho u(z) b dz = \frac{\rho}{2\eta} \frac{dp}{dx} \left(\frac{h^2}{6} + \delta h \right),$$

The real relationship between the pressure gradient and the flow rate in MD simulated nanoflows is not known. Therefore a comparison of the friction coefficient obtained by MD simulation and from hydrodynamics is performed for equal pressure gradients or flow rates. This comparison is presented in Figure 3. Here the solid line corresponds to the hydraulic resistance coefficients $\lambda_h = 24/Re$ and the dashed line to the MD data. Both curves have the similar qualitative dependences on the Reynolds number but the hydrodynamic values are higher. It should be noted that this data are obtained only for small Reynolds data. On the other hand, these Reynolds numbers are typical for nanoflows.

Another interesting graph (see Figure 4) shows the dependence of the resistance coefficient on the Knudsen number.

4. THE FLUID STRUCTURE IN PLANE CHANNEL

In spite of the disadvantages of the previous MD algorithms noted in the introduction, many interesting results have been obtained by these techniques. In particular, it has been shown

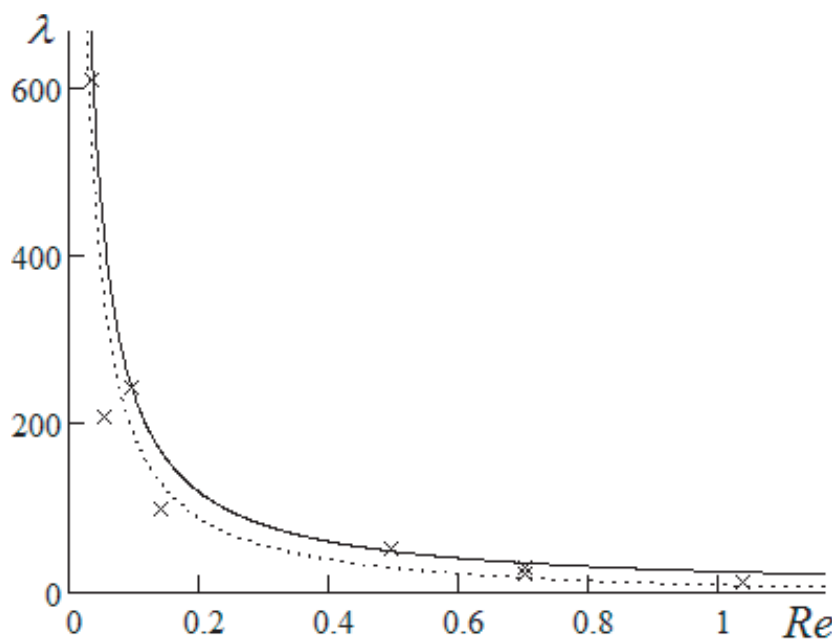


Figure 3. Resistance coefficient versus the Reynolds number. Crosses correspond to MD data. Dashed line is approximation of MD data. Solid line is the hydraulic resistance coefficients.

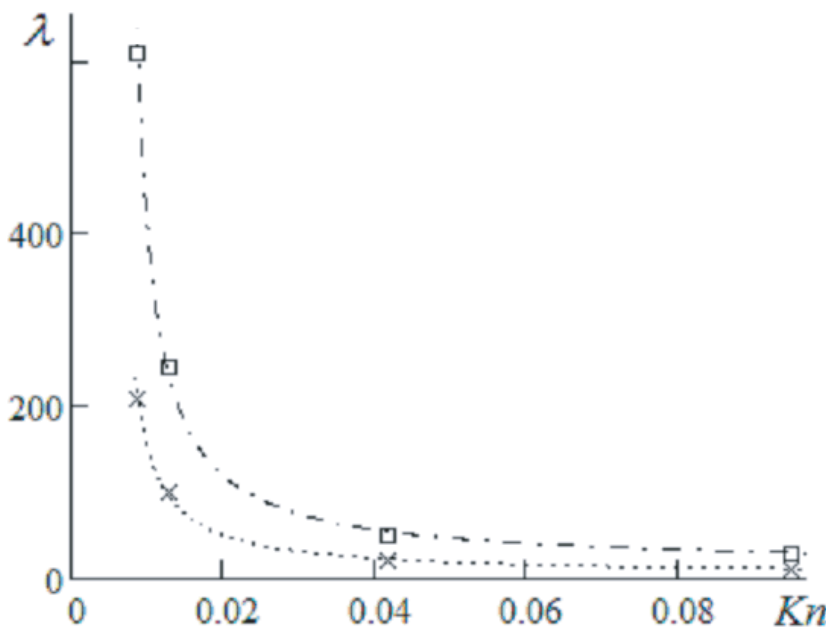


Figure 4. Resistance coefficient versus the Knudsen number. Crosses correspond to MD data ($\theta = 0.5$), box labels – to MD data ($\theta = 1$).

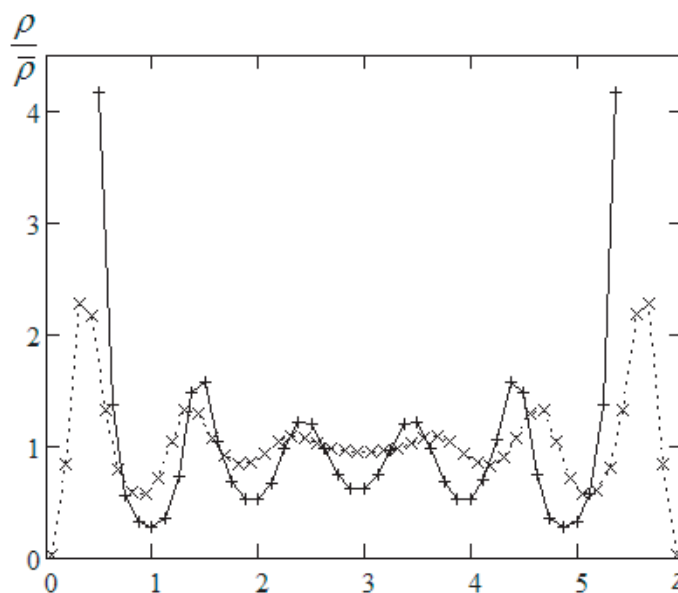


Figure 5. The density profiles across the channel for HS (+), and LJ fluid (×). $L = 60\sigma$, $h = 6\sigma$, $\varepsilon_v = 0.79$

that the fluid density profile in a nanochannel is inhomogeneous [1]. The maximum fluid density is recorded near the walls. However, the HS fluid flow has not previously been modeled. Density profiles in the channel cross section for LJ and HS fluids are compared in Figure 5. A well-defined periodic structure is observed. It is evident that the largest values of the density maxima are observed at the channel walls. The number and height of the maxima increase with increasing fluid density. The periodic structure is more pronounced in a HS fluid than in a LJ fluid at the same average density. This is primarily due to the existence of a screening layer at the walls for such fluid, the layer thickness being equal to the radius of the molecules. For LJ molecules, the screening effect is less pronounced because the LJ potential is softer than the HS potential and the molecules can theoretically move arbitrarily close to the boundary. As a consequence, for a hard-sphere fluid, the effective volume occupied by the fluid is smaller and, hence, the average density is higher and the structuring effect is stronger than those for a LJ fluid. Because of the existence of the screening zones the effective volume occupied by the LJ molecules is more than that occupied by the HS molecules. Therefore the effective density of the HS fluid is higher than density of LJ molecules (at the same number of molecules in the modeling cell!). But the fluid structuring in channel increases with grows of the fluid density.

Fluid structuring in a nanochannel is of fundamental importance. However this structuring decreases along the channel. The fluid concentration field along the channel is given in Figure 6 (here the dense regions are lighter gray). The structure of the density field changes significantly along the channel, and the average fluid density decreases with increasing longitudinal coordinate. The fluid is compressible but its Knudsen number is rather large (for fluid in Figure 6 $Kn = 1.3 \cdot 10^{-2}$).

Because the flow rate is constant, the density drop along the channel results in an increase in the average flow velocity. In this sense, a very interesting situation occurs. Roughly speaking the flow parameters are changed from section to section, i.e., the flow field is non-



Figure 6. Typical density field along the nanochannel. $L = 60\sigma$, $h = 6\sigma$, $\varepsilon_v = 0.79$

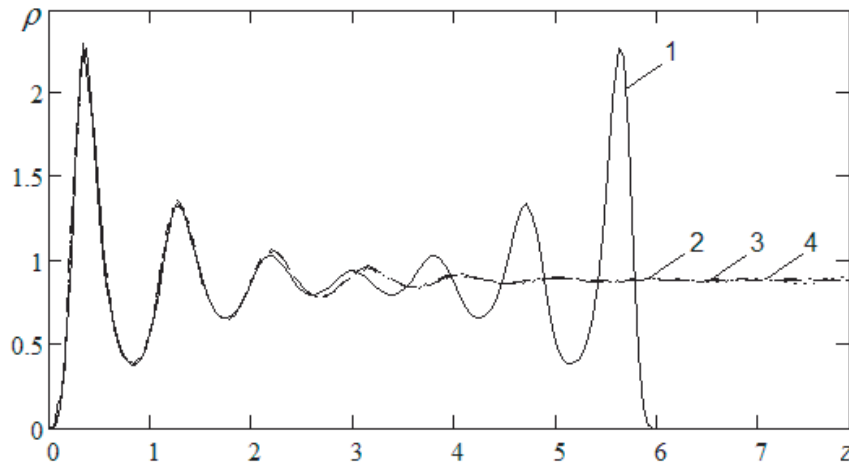


Figure 7. Density profiles for nanochannels with different heights. $\varepsilon_v = 0.88$, 1 - $h = 6\sigma$, 2 - $h = 12\sigma$, 3 - $h = 24\sigma$, 4 - $h = 48\sigma$

stationary but is periodic with the period L/\bar{v} . Thus we have specific quasi-stationary flow. The density variation is due to a pressure drop. The average fluid density remains constant only for specular reflection of the HS molecules.

It should be emphasized that the order of the fluid near the walls is a characteristic feature of nanochannel flows and it does not disappear with increasing distance between the channel walls. This is illustrated in Figure 7, which shows fluid density profiles across channels of various heights. Here curve 1 corresponds to the height $h = 6\sigma$, the curve 2 to $h = 12\sigma$, curve 3 to $h = 24\sigma$, and curve 4 to $h = 48\sigma$. Fluid structuring in the channel practically does not depend on the channel height if the latter is greater than 10σ . In all cases, appreciable structuring takes place at a distance from the walls of about $5-6\sigma$.

Velocity profile gives the local information on the fluid structure. However, an analysis of the Figs. 5-7 shows that the short-range order of the fluid in a nanochannel varies. It should be appreciable at least near the walls. The character of the fluid structure is detected by the radial distribution function of the molecules. Figure 8 shows radial distribution functions in an open system (solid line) and at the first density maximum (see Figure 5) in a nanochannel (dotted line). The distance r is in the units of σ . It is evident that the magnitude and number of maxima in the channel are significantly increased compared to the open system, indicating an increase in the short-range order in the fluid due to its interaction with the walls. Near the

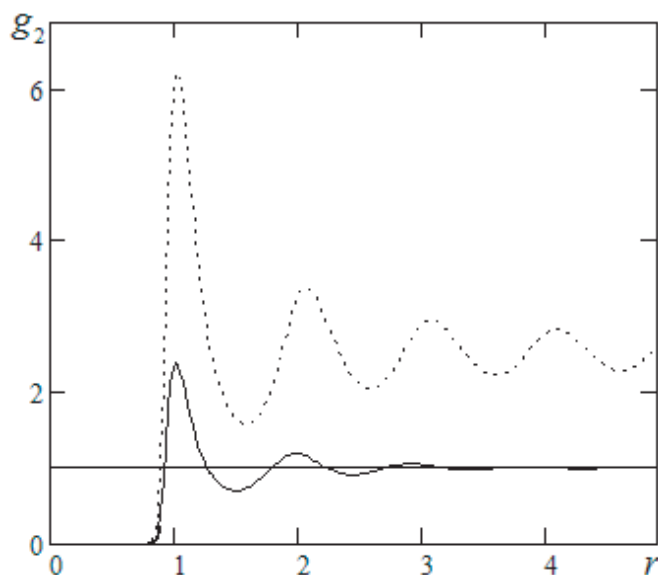


Figure 8. Radial distribution function g_2 in an open system (solid curve) and in a nanochannel at the first density maximum (dashed curve). $h = 6\sigma$, $\epsilon v = 0.88$

wall the radial distribution function decays over a distance an order of magnitude larger than in bulk. In fact, quasi-long-range order is observed near the wall.

Information on the fluid structure over the entire channel can be obtained using the space pair distribution function of molecules (see Figure 9).

5. CONCLUSION

The MD algorithm developed in the present study is suitable for modeling plane fluid flow with a linear pressure gradient which is a macroscopic analog of stationary Poiseuille flow. Unlike in Poiseuille flow, the MD flow is not stationary in standard sense. Its parameters vary along the channel. In particular, the fluid density decreases with increasing longitudinal coordinate. The fluid behaves like a compressible gas even if its density corresponds to density of liquid. The fluid compressibility is observed only if a pressure drop takes place. The fluid is incompressible if its molecules are specularly reflected from the wall. Thus, a pressure drop is caused by diffuse or specular-diffuse reflection of the fluid molecules.

The flows of HS and LJ fluids are qualitatively similar. There is the pressure drop in both cases. The value of pressure drop for the LJ fluid flow is determined by the parameters of the interaction potential between the fluid and wall molecules. There are parameters for which the characteristics of both fluids coincide. This provides an opportunity for determining accommodation coefficients [11].

Interaction of the molecules with the wall changes the fluid structure in the channel. In near-wall zone the fluid density is higher than the average value. Thus, near the wall there is a fluid nano-layer with special properties. The fluid in this layer is structured, and quasi-long order of the fluid is observed near to wall. The character of this structuring is almost independent of the channel height. Apparently, the existence of this layer determines the slip length under ideal conditions (absolutely smooth walls). This layer plays the role of a

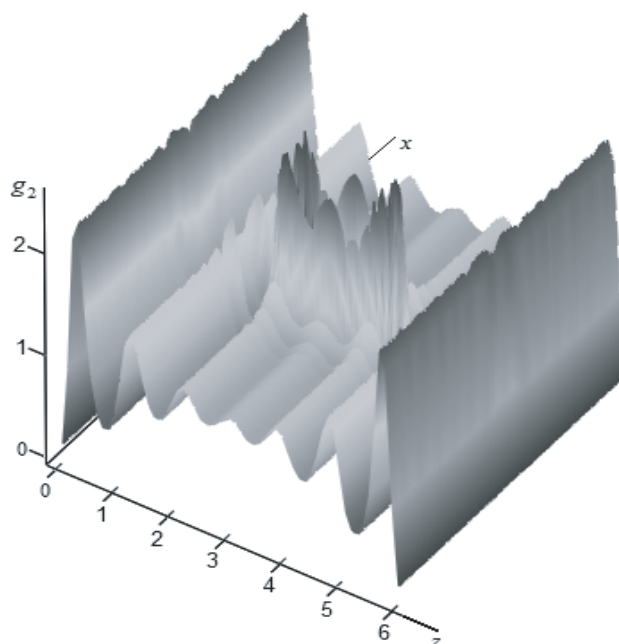


Figure 9. Space radial distribution function for a molecule on the axis of the nanochannel. $h = 6\sigma$, $\varepsilon_v = 0.88$

Knudsen layer in the rarefied gas. However, the existence of this layer does not explain the slip lengths observed in real experiments. Large values of the slip length may be attributed to the wall roughness. Investigation of this problem is an important challenge of the physics of microflows.

ACKNOWLEDGEMENTS

This work was supported in part by the Russian Foundation for Basic Researches (grant No. 10-01-00074) and by the Federal Special Program of Russian Federation “Scientific and scientific-pedagogical personnel of innovative Russia in 2009-2013” (contracts No. P230, No. 14.740.11.0579).

REFERENCES

- [1] G. Karnidakis, A. Beskok, N. Aluru. *Microflows and nanoflows. Interdisciplinary Applied Math. Springer Science+Business Media, Inc.* 2005. V. 29. 817 p.
- [2] J.O. Hirschfelder, Ch.F. Curtiss, R.B. Bird. *Molecular Theory of Gases and Liquids*, John Wiley and Sons, Inc., 1954.
- [3] L. Xu, M.G. Sedigh, M. Sahimi, T.T. Tsotsis. Nonequilibrium molecular dynamics simulation of transport of gas mixtures in nanopores. *Phys. Rev. Lett.*, 1998, 80, 3511–3514.
- [4] P. Schofield. Computer simulation studies of the liquid state. *Comput. Phys. Comm.*, 1973, 5, 17–23.
- [5] D.C. Rapaport. *The art of molecular dynamics simulation*, Cambridge University Press, 2005.
- [6] V.N. Kogan. *Rarefied gas dynamics*, Plenum Press, 1969.
- [7] E. Lauga, M.P. Brenner, H.A. Stone. *Microfluidics: the no-slip boundary condition. Handbook of Exper. Fluid Dynamics*. Ch. 19. N.Y.: Springer, 2007, 1219–1240.
- [8] J. Ou, B. Perot, J.P. Rothstein. Laminar drag reduction in microchannels using ultrahydrophobic surfaces.

Phys. Fluids, 2004, 16(12), 4635–4643.

- [9] E.T. Watts, J. Krim, A. Widom. Experimental observation of interfacial slippage at the boundary of molecularly thin films with good substrate. *Phys. Rev. B*, 1990, 41(6), 3466–3472.
- [10] N. De Nevers. *Fluid Mechanics*, Addison-Wesley, 1970.
- [11] V. Rudyak, A. Belkin, V. Egorov, D. Ivanov. Modeling of plane flow with a pressure gradient in a nanochannel. In *Proc. of 1st European Conference on Microfluidics*. Bologna: CHF (CDROM). 2008. μ FLU08-38.

